AUT Journal of Electrical Engineering

AUT J. Elec. Eng., 54(2) (2022) 295-312
DOI: 10.22060/eej.2022.21387.5472

Unbalanced Voltage Compensation Using Grid-Connected Photovoltaic System

A. Mohammadi, Sh. Karimi*, H. Moradi Cheshmehbeigi

Department of Electrical Engineering, Razi University, Kermanshah, Iran

ABSTRACT: Appropriate power quality is indispensable for electrical distribution networks, especially in microgrids including renewable energy sources. One of the critical issues affecting power quality is the unbalanced voltage. Voltage imbalance in microgrids spreads due to proximity of loads and power sources, causing instability, and eventually interruption. In general, unbalanced voltage can be compensated by using reactive power compensators, e.g. series active power filter and dynamic voltage restorer. However, these equipment imposes additional costs, which is not economically viable. Recently, the surplus capacity of inverter-interfaced Distributed Generations is used to improve voltage quality. In this regard, the control methods based on Proportional-Resonance controllers in αβ frame or PI controllers in a Dual-frame Synchronous Reference Frame (DSRF) are the usual methods that are used. The problem of limiting the output current in αβ frame and the problem of oscillating components in DSRF are the weakness of these methods. To resolve the mentioned drawbacks, a control method based on Decoupled Double Synchronous Reference Frame (DDSRF) is proposed in this paper for unbalanced voltage compensation, using a two-stage grid-connected Photovoltaic system. The simulation results show that despite the dynamic changes and the alternating nature of the Photovoltaic system in power generation, the proposed control system appropriately compensates the unbalanced voltage, and controls the DC link voltage and the Photovoltaic output power. After compensation using the proposed control strategy, the Voltage Unbalance Factor (VUF) and the Total Harmonic Distortion (THD) at the PCC are under the permissible range accounting for two percent and five percent, respectively.

Review History:

Received: May, 10, 2022
Revised: Jul. 01, 2022
Accepted: Jul. 16, 2022
Available Online: Dec. 01, 2022

Keywords:

Grid-connected Photovoltaic system
Decoupled Double Synchronous Reference Frame
unbalanced voltage compensation,
Voltage Unbalance Factor.

1- Introduction

Today, the penetration of renewable energy sources is increasing due to climate change, increasing production of environmental pollutants, decreasing energy sources, and the rising trend of fossil fuel prices in the world energy market. Due to the growth of energy consumption and the cost of constructing new transmission lines, Distributed Generation (DG) units have become increasingly crucial to response to the requirements of energy consumers. One of the renewable resources of DGs is solar energy. Solar power plants can be considered a suitable option to replace fossil fuel power plants [1-3].

In Photovoltaic (PV) based DG units, the output power is intermittent due to changes in environmental conditions. On the other hand, appropriate power quality is indispensable, especially in microgrids. One of the critical issues affecting power quality is an unbalanced voltage problem. Voltage imbalance mainly happens due to unbalanced distribution of single-phase and nonlinear loads or grid faults. Unbalanced voltage in microgrids spreads due to proximity of loads and power sources, causing instability and ultimately microgrid disruption [4, 5]. On the other hand, due to the low inertia of DG sources and the high speed of power electronic instruments, the dynamics of the microgrids are much faster than the dynamics of conventional power systems, which multiply the probability of instability and voltage collapse [6, 7].

In general, unbalanced voltage can be compensated by different methods. We can mention these ways in compensation methods: using series active power filters and dynamic voltage restorers [8-10], injection of negative sequence currents into the system by parallel active filters [11], and using parallel-series compensators such as the unified power quality conditioner [12, 13]. The static synchronous compensator is another solution for unbalanced voltage compensation. In this method, voltage compensation at the desired point is done by injecting positive and negative sequences of reactive power [14, 15]. The use of the methods mentioned for unbalanced voltage compensation imposes additional costs on the system, which is not economically viable. Authors in [16] develop a reactive power compensation strategy that uses single-phase distributed PV inverters to mitigate voltage unbalance. However, the proposed control method requires infrastructure communications. In [17], the control system is designed hierarchically at primary and secondary levels. The secondary level controller acts as the central controller, and

*Corresponding author's email: shahramkarimi@razi.ac.ir

sends appropriate control signals to the primary level controllers to compensate for the unbalanced voltage at PCC. Two methods for controlling the interface converter of a grid-connected DG system for unbalanced voltage compensation are presented in [18]. The first method decreases the active power oscillation under unbalanced voltage conditions, and the second method focuses on controlling the negative sequence components of the current. In [19], the negative component impedance control loop at the unbalanced load connection point is used to improve the microgrid performance during unbalanced conditions. A three-level control method for unbalanced voltage compensation and microgrid performance improvement is presented in [20]. The first level of the control system has the task of controlling the negative sequence components for adequate power sharing, the second level has the duty of the unbalanced compensation, and finally the third level has the task of improvement of power quality. In [17] to [20], methods for unbalanced voltage compensation in the αβ frame have been performed by Proportional-Resonance (PR) controllers. When the control system is implemented in the αβ frame, it is impossible to use a current limiter in the control system due to the sinusoidal current sources, which can damage converter during an overload or grid fault.

Therefore, the researchers have proposed using PI controllers in a Dual-frame Synchronous Reference Frame (DSRF) control system [21, 22]. Nevertheless, DSRF cannot effectively distinct the positive and negative sequence components and causes the oscillating components in the d-q frame. In [23] and [24], low-pass filters are used to reduce the oscillating components and improve system performance. Moreover, low-pass filters do not entirely remove these oscillations and cause dynamic response slowing. In [25], Decoupled Double Synchronous Reference Frame (DDSRF) is proposed to eliminate these oscillatory signals. However, in [25], the reference current is assumed to be DC, which in most conditions is not the case. In [26], a DDSRF-based method is proposed for unbalanced voltage compensation in a stand-alone microgrid. Moreover, in [26], an ideal constant DC source is considered .as a DC part, and the DC link dynamic is not considered

This paper presents an effective control method for a two-stage grid-connected Photovoltaic system to compensate for unbalanced voltage at PCC caused by unbalanced loads. DDSRF has been used to properly separate the sequence components. Despite the dynamic and intermittent nature of the PV system, the proposed control system appropriately controls DC link voltage, and PV output power. Using the proposed control strategy, the Voltage Unbalance Factor (VUF) at PCC falls within its permissible range.

In the rest of the paper, the proposed DDSRF method is presented in section 2. In section 3, the proposed control system of a two-stage grid-connected PV system is described. The grid-connected Photovoltaic system and its control system are simulated using SimPowerSystem/Simulink, and the simulation results are shown in section 4. Finally, the conclusion is presented in section 5.

2- DDSRF Structure

For unbalanced voltage compensation, the negative sequence components of voltage must be eliminated. Thus, the negative sequence components must first be separated from the positive sequence components. DDSRF has been used to better separate these sequence components, which will be discussed in the following. Fig. 1 illustrates the positive and negative sequence components of the unbalanced voltage vector in the DSRF, comprising a rotating frame dq^+ with the angular speed ω,' the angular displacement θ', a rotating frame dq^- with the angular speed of -ω', and the angular displacement of -θ'. Assuming that the angular displacement of the frame dq^+ is equal to the angular displacement of the positive sequence components of the voltage vector θ›=ωt, the unbalanced voltage vector is expressed as follows:

$$v_{dq}^{\pm}=\begin{bmatrix}v_d^{\pm}\\ v_q^{\pm}\end{bmatrix}=\left[T_{dq}^{\pm}\right].v_{\alpha\beta}=V^{\pm}\begin{bmatrix}1\\0\end{bmatrix}+V^{\mp}\begin{bmatrix}\cos(\mp 2\omega t)\\ \sin(\mp 2\omega t)\end{bmatrix} \quad (1)$$

Where:

$$\left[T_{dq}^{+}\right]=\left[T_{dq}^{-}\right]^{T}=\begin{bmatrix}\cos(\theta') & \sin(\theta')\\ -\sin(\theta') & \cos(\theta')\end{bmatrix} \quad (2)$$

It can be seen that the voltage sequence components in the d-q frame comprise a dc part and a double frequency oscillating part. To better separate the sequence components and eliminate the oscillating part, the DDSRF method is used.

If we consider the unbalanced voltage and current as follows:

$$v_{\alpha\beta}=\begin{bmatrix}v_\alpha\\ v_\beta\end{bmatrix}=v_{\alpha\beta}^{+}+v_{\alpha\beta}^{-}=V^{+}\begin{bmatrix}\cos(\omega t+\phi^{+})\\ \sin(\omega t+\varphi^{+})\end{bmatrix}+V^{-}\begin{bmatrix}\cos(-\omega t+\phi^{-})\\ \sin(-\omega t+\varphi^{-})\end{bmatrix} \quad (3)$$

$$i_{\alpha\beta}=\begin{bmatrix}i_\alpha\\ i_\beta\end{bmatrix}=i_{\alpha\beta}^{+}+i_{\alpha\beta}^{-}=I^{+}\begin{bmatrix}\cos(\omega t+\delta^{+})\\ \sin(\omega t+\delta^{+})\end{bmatrix}+I^{-}\begin{bmatrix}\cos(-\omega t+\delta^{-})\\ \sin(-\omega t+\delta^{-})\end{bmatrix} \quad (4)$$

Using the equations $i_{dq}^{\pm}=e^{-J\theta^{\pm}}.i_{\alpha\beta}^{\pm}$ and $v_{dq}^{\pm}=e^{-J\theta^{\pm}}.v_{\alpha\beta}^{\pm}$, positive sequence components of voltage and current can be expressed by separating dc and oscillating parts in the d-q frame:

$$\boldsymbol{v}_{dq}^{\pm}=\underbrace{\bar{\boldsymbol{v}}_{dq}^{\pm}}_{DC}+\underbrace{e^{-J(\pm 2\omega t+\varphi^{\pm}-\varphi^{\mp})}\bar{\boldsymbol{v}}_{dq}^{\mp}}_{AC} \quad (5)$$

$$\boldsymbol{i}_{dq}^{\pm}=\underbrace{\bar{\boldsymbol{i}}_{dq}^{\pm}}_{DC}+\underbrace{e^{-J(\pm 2\omega t+\delta^{\pm}-\delta^{\mp})}\bar{\boldsymbol{i}}_{dq}^{\mp}}_{AC} \quad (6)$$

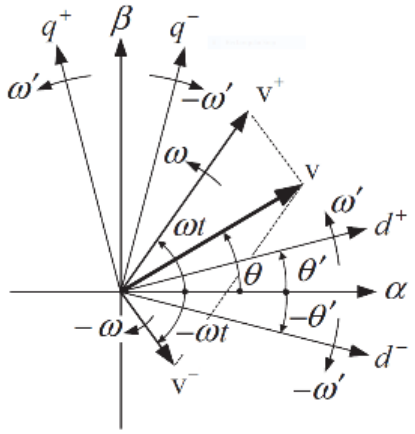

Fig. 1. Voltage vector in DSRF and separation of positive and negative sequence components [27]

As seen in equations (5) and (6), there is an oscillating part with twice the frequency of the grid frequency between the positive and negative d-q axes. Using the DDSRF method, the sequence components decoupled by subtracting the oscillating part of the positive and negative sequence components, as follows:

$$v_{dq}^{\pm} = \underbrace{\bar{v}_{dq}^{\pm}}_{DC} + \underbrace{e^{-J(\pm 2\omega t+\varphi^{\pm}-\varphi^{\mp})}\bar{v}_{dq}^{\mp}}_{AC} - \underbrace{e^{-J(\pm 2\omega t+\varphi^{\pm}-\varphi^{\mp})}\bar{v}_{dq}^{\mp}}_{Decoupling-term} \quad (7)$$

$$i_{dq}^{\pm} = \underbrace{\bar{i}_{dq}^{\pm}}_{DC} + \underbrace{e^{-J(\pm 2\omega t+\delta^{\pm}-\delta^{\mp})}\bar{i}_{dq}^{\mp}}_{AC} - \underbrace{e^{-J(\pm 2\omega t+\delta^{\pm}-\delta^{\mp})}\bar{i}_{dq}^{\mp}}_{Decoupling-term} \quad (8)$$

In Fig. 2, the block diagram of the sequence components extraction based on the DDSRF method for both voltage and current is shown. In this figure, the NF block is the notch filter that is tuned to eliminate the oscillating part. The block diagrams of the decoupling blocks are presented in Figs. 2c and 2d.

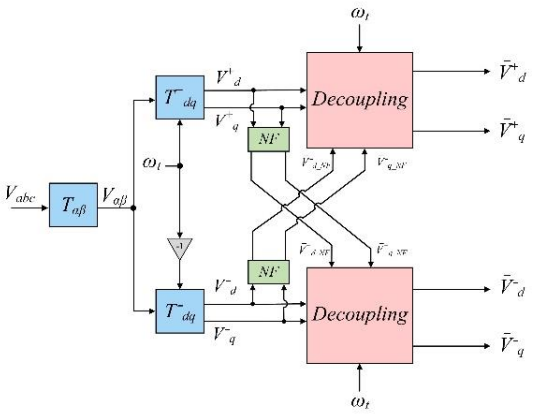

a)

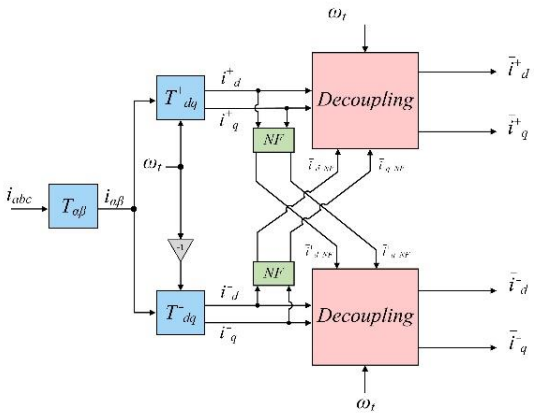

b)

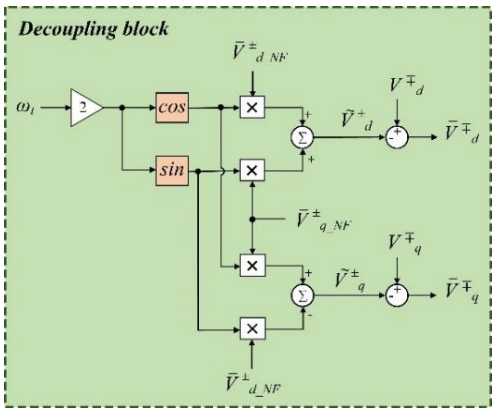

c)

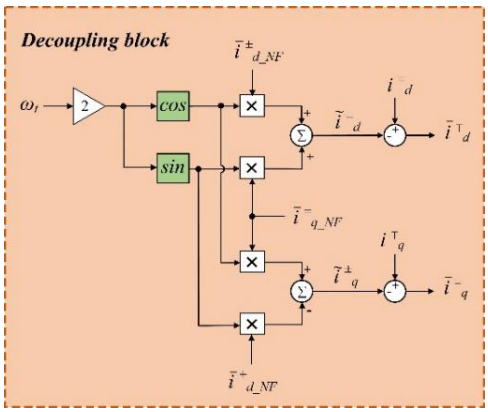

d)

Fig. 2. Block diagram of sequence components extraction based on DDSRF method a) voltage components, b) current components c) voltage decoupling block d) current decoupling block

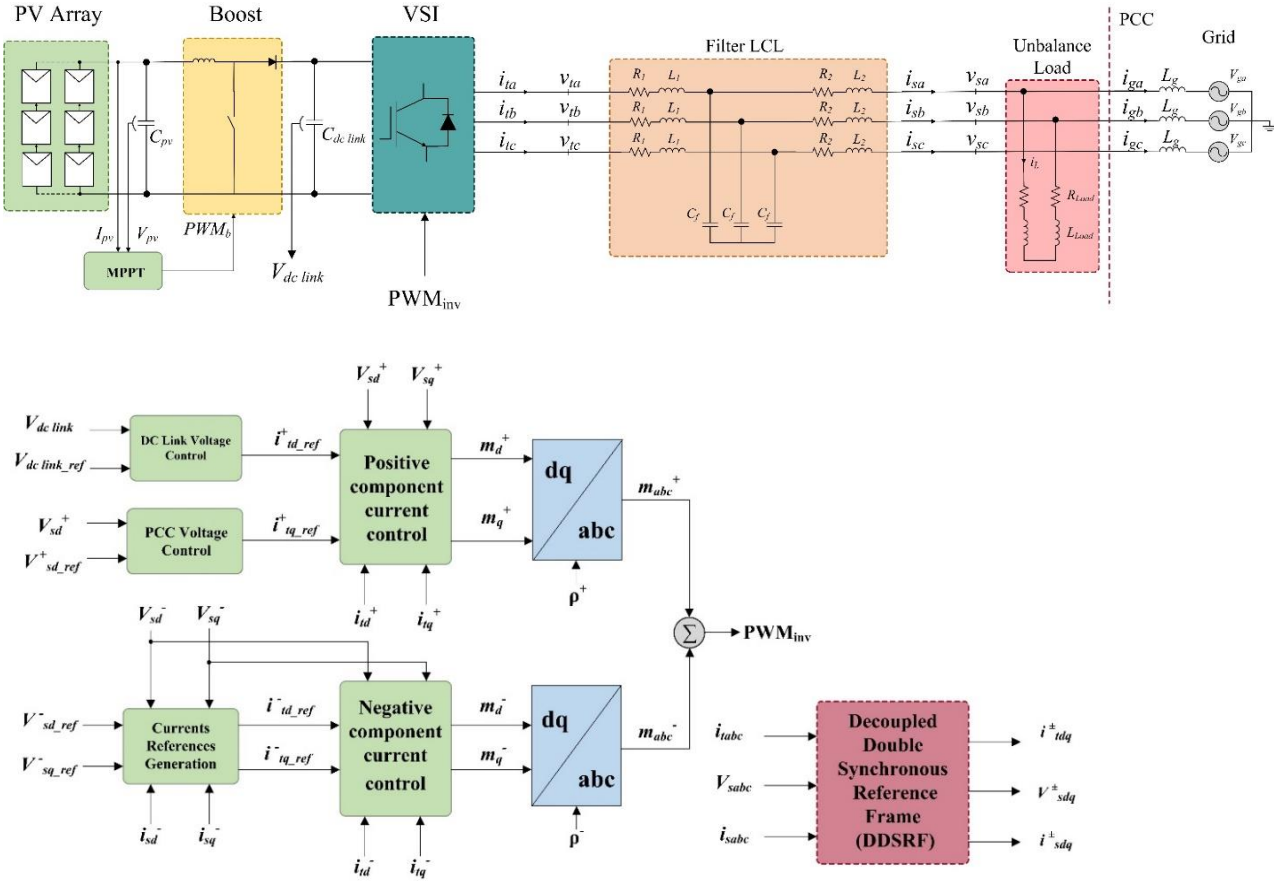

Fig. 3. Structure and block diagram of the proposed control strategy of a two-stage grid-connected PV system.

3- Proposed Control Strategy

In a two-stage grid-connected PV system, power control is done by controlling two converters. In the proposed control strategy, the DC-DC converter controls the power extracted from the Photovoltaic panels via MPPT control algorithm, and the voltage source inverter controls the output active power and compensates the unbalanced PCC voltage simultaneously. The main focus of this paper is on the inverter control under unbalanced load conditions. The proposed inverter control system has one inner and two outer control loops. The outer control loops include the DC link and PCC voltage control that produce the reference currents for the inner control loop. The inner control loop is a current controller that controls the inverter output currents. To adequately separate the positive and negative sequence components of the voltage and current signals, DDSRF is used. Fig. 3 shows the overall structure of the proposed control strategy for the two-stage grid-connected PV system.

3- 1- DC Link Voltage Control Loop

To inject the active power generated by PV system into the grid, the DC link voltage must be controlled. The dynamic of the power exchanged between the DC link, and the PV system can be expressed as follows:

$$\left(\frac{C_{dc\_link}}{2}\right)\frac{dV_{dc\_link}^{2}}{dt} = P_{pv} - P_{dc} \tag{9}$$

Where, P_{pv} is the PV output power and P_{dc} is the DC link output power.

Ignoring the losses, the inverter output power, P_t, can be considered equal to P_{dc}. Therefore, the inverter output power is equal to the PV output power if the DC link voltage is regulated. Fig4 . depicts the DC link voltage controller. The inverter output active and reactive power under unbalanced conditions can be described as follows:

$$P_t^{+}(t) = \frac{3}{2}\left[V_{td}^{+}(t)i_{td}^{+}(t) + V_{tq}^{+}(t)i_{tq}^{+}(t)\right] \tag{10}$$

$$Q_t^{+}(t) = \frac{3}{2}\left[-V_{td}^{+}(t)i_{tq}^{+}(t) + V_{tq}^{+}(t)i_{td}^{+}(t)\right] \tag{11}$$

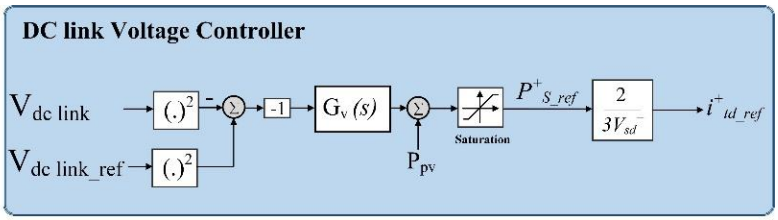

Fig. 4. Block diagram of the DC link voltage control system.

In the steady state, $V_{tq}^{+}=0$, the positive sequence components of the reference current in the d-q axes can be obtained as follows:

$$i_{td\_ref}^{+}(t)=\frac{2}{3V_{sd}^{+}}P_{t\_ref}^{+}(t) \tag{12}$$

$$i_{tq\_ref}^{+}(t)=\frac{-2}{3V_{sd}^{+}}Q_{t\_ref}^{+}(t) \tag{13}$$

According to equations (12) and (13), the active and reactive power can be controlled by the positive sequence components of the reference current in the d-q axes.

3- 2- Unbalanced Voltage Compensation

To compensate for the unbalanced PCC voltage, the negative sequence components of the PCC voltage should be eliminated. These components can be eliminated using appropriate negative sequence components of the current generated by the inverter.

By applying Kirchhoff's current law at the LCL filter and converting the equations to the negative d-q frame, the following equations are achieved:

$$C_f\frac{dV_d^{-}(t)}{dt}=i_{td}^{-}(t)-i_{sd}^{-}(t)-C_f\omega(t)V_{sq}^{-}(t) \tag{14}$$

$$C_f\frac{dV_q^{-}(t)}{dt}=i_{tq}^{-}(t)-i_{sq}^{-}(t)+C_f\omega(t)V_{sd}^{-}(t) \tag{15}$$

The control commands of the negative sequence components, u_{vd}^{-} and u_{vq}^{-} can be obtained after Laplace transformation:

$$i_{td}^{-}=u_{vd}^{-}+C_f\omega V_{sq}^{-}+i_{sd}^{-} \tag{16}$$

$$i_{tq}^{-}=u_{vq}^{-}-C_f\omega V_{sd}^{-}+i_{sq}^{-} \tag{17}$$

Equations (16) and (17) show that by adding and subtracting $C_f\omega V_{sq}^{-}$ and $C_f\omega V_{sd}^{-}$, the components in the d-q axes can be decoupled. As a result, the negative sequence components of the reference current are generated, as presented in Fig. 5. The closed-loop transfer function of the current controller, which is explained in subsection 3.3, can be expressed as follows:

$$G_i(s)=\frac{i_{tdq}^{\pm}(s)}{i_{tdq\_ref}^{\pm}(s)}=\frac{1}{\tau_i s+1} \tag{18}$$

where, τ_i is the time constant of the current controller.

According to Fig. 5, the open-loop transfer function of the control loop for unbalanced voltage compensation can be written as follows:

$$L_v(s)=G_{vdq}^{-}(s)\left(\frac{1}{C_f s}\right)\left(\frac{1}{\tau_i s+1}\right) \tag{19}$$

where $G_{vdq}^{-}(s)$ can be considered as a proportional controller [28]:

$$G_{vdq}^{-}(s)=k_{pv-dq^{-}} \tag{20}$$

It is worth noting that $V_{sd\_ref}^{-}$ and $V_{sq\_ref}^{-}$, which are the negative sequence components of the reference voltage in the d-q frame, are zero.

Additionally, the amplitude of PCC voltage is regulated by injecting an adequate value of the reactive power. Fig. 6 shows the block diagram of the control system related to the PCC voltage regulation. In this figure, $V_{sd\_ref}^{+}$ is the desired voltage amplitude. The compensator $K_{vac}(s)$ can be considered as a PI controller. The compensator parameters are determined based on the gain and phase margin requirements, and the desired bandwidth of the control system.

$$K_{vac}(s)=k_{p\_vac}+\frac{k_{i\_vac}}{s} \tag{21}$$

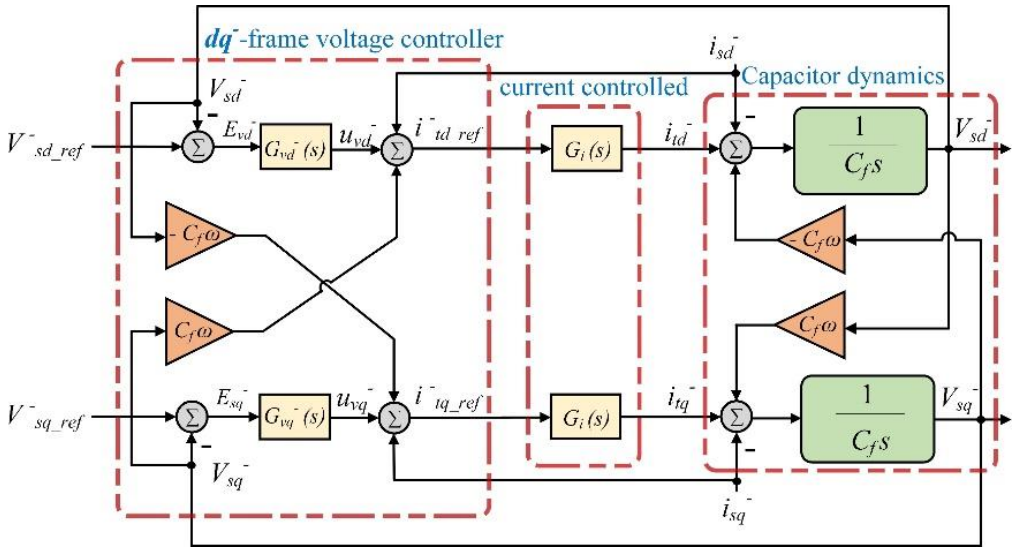

Fig. 5. Control loop for unbalanced voltage compensation.

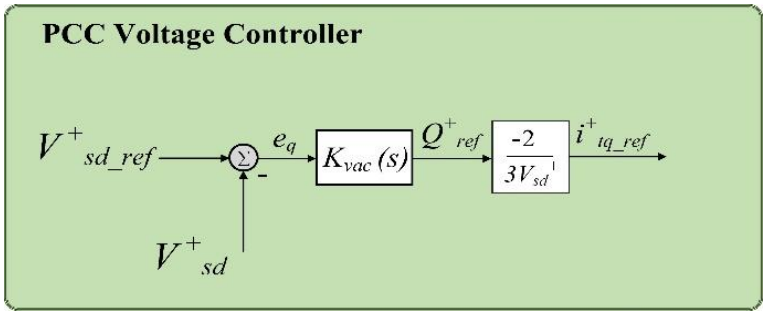

Fig. 6. Block diagram of the PCC voltage regulator

3- 3- Current Control Loop

By separating the positive and negative sequence components using the proposed DDSRF, the inverter AC side dynamic in the positive, and negative reference frames are given as follows:

$$L_t \frac{di^+_{tdq}(t)}{dt} = -R_t i^+_{tdq}(t) \pm L_t \omega i^+_{tqd}(t) + V^+_{tdq}(t) - V^+_{sdq}(t) \quad (22)$$

$$L_t \frac{di^-_{tdq}(t)}{dt} = -R_t i^-_{tdq}(t) \mp L_t \omega i^-_{tqd}(t) + V^-_{tdq}(t) - V^-_{sdq}(t) \quad (23)$$

where $L_t = L_1 + L_2$ and $R_t = (R_1 + r_{on}) + R_2$ are the inductance value and AC side resistance, respectively.

As seen in equations (22) and (23), d and q-axes currents are coupled. To decouple these currents and by using the equations $V_{tdq}{}^+(t) = \frac{V_{dclink}}{2}.m_{dq}{}^+$ and $V_{tdq}{}^-(t) = \frac{V_{dclink}}{2}.m_{dq}{}^-$, the control signals are considered as follows:

$$m_{dq}{}^+ = \frac{2}{V_{dc\_link}}\left(u_{dq}{}^+ \mp L_t \omega i^+_{tqd} + \right)V^+_{sdq} \quad (24)$$

$$m_{dq}{}^- = \frac{2}{V_{dc\_link}}\left(u_{dq}{}^- \pm L_t \omega i^-_{tqd} + \right)V^-_{sdq} \quad (25)$$

where $u_{dq}{}^+$ and $u_{dq}{}^-$ are the control signals. Fig. 7 illustrates the block diagram of the current controller in d-q reference frame. The open-loop transfer function of this control

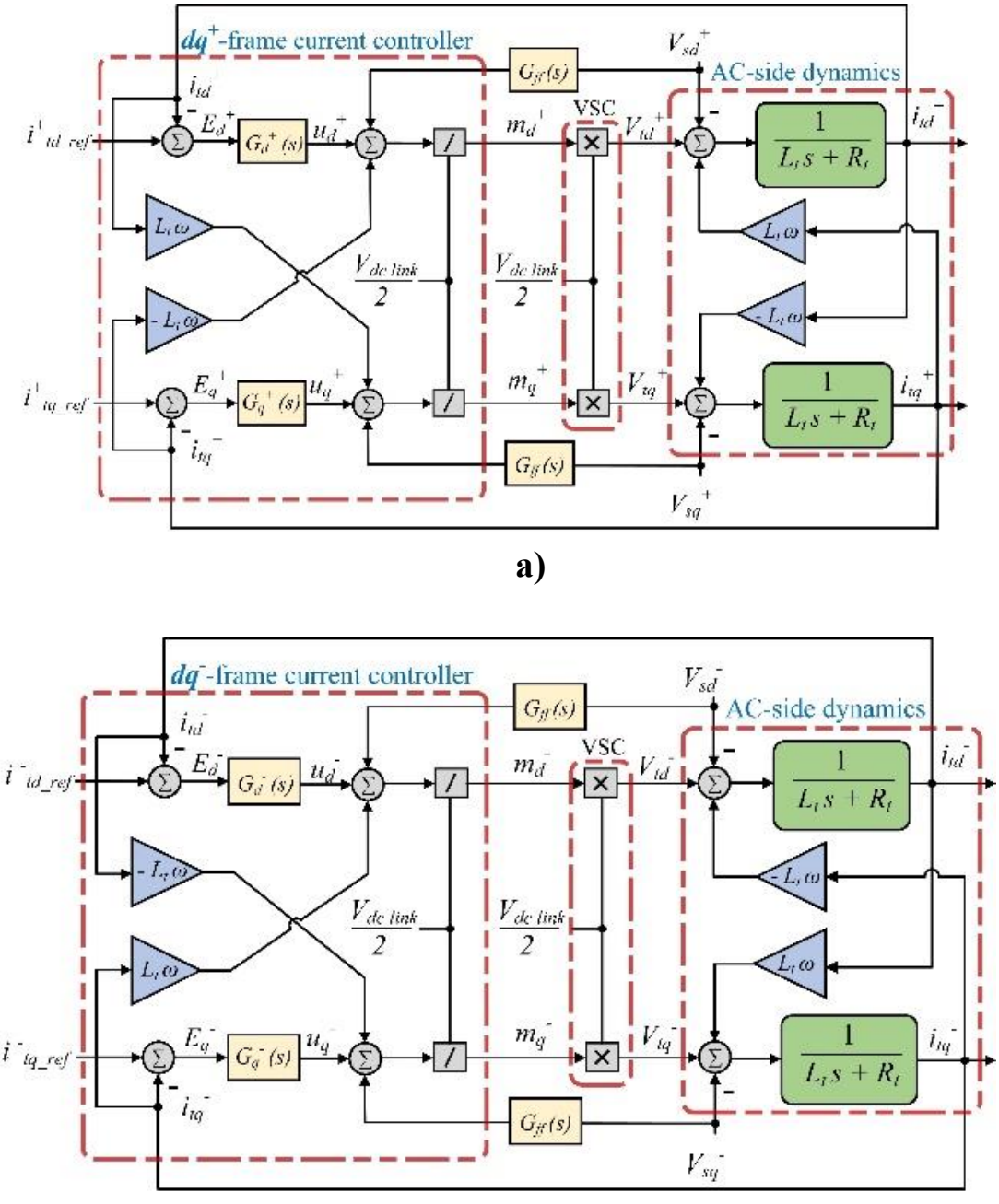

a)

b)

Fig. 7. Block diagram of the current controllers a) positive sequence components, b) negative sequence components

system can be expressed as follows:

$$L_I(s) = G_{dq}^{\pm}(s)\left(\frac{1}{\tau_i s + 1}\right) \tag{26}$$

where $G_{dq}^{\pm}(s)$ can be considered as a PI controller:

$$G_{dq}^{\pm}(s) = k_{pdq^{\pm}} + \frac{k_{idq^{\pm}}}{s} \tag{27}$$

Table 1. Specification of the PV system [29]

Parameter	value
maximum power, P_{pv}	2.86MW
voltage at MPP, V_{mpp}	1368 V
current at MPP, I_{mpp}	2093 A
number of series modules, n_s	25
number of parallel modules, n_p	375
PV capacitor, C_{pv}	80 µF

Table 2. Studied system parameters [28]

Parameter	value
boost converter inductance, L_b	738 µH
boost converter resistance, R_b	5 mΩ
switching frequency, f_{sw}, f_b	5 kHz
DC link capacitance, $C_{dc\text{-}link}$	700 µF
DC link voltage, $V_{dc\text{-}link}$	2500 V
inverter side inductance, L_1	350 µH
inverter side resistance, R_1	2.38 mΩ
filter capacitor, C_f	2500 µF
grid side inductance, L_2	2 µH
grid side resistance, R_2	0.1 mΩ
amplitude of voltage, V_s	391 V
angular frequency, ω	377 rad/s
grid inductance, L_g	50 µH

4- Studied System and Simulation Results

The system under study is a two-stage grid-connected PV system. Specifications of the PV module are presented in Table 1. The system parameters and the control system parameters are shown in Table 2 and Table 3, respectively. The load is a switchable Y-connection load with the impedance of 0.1 + j0.01 Ω/phase, which each phase can separately disconnect or connect to the system.

The grid-connected PV system and the proposed control scheme have been simulated using the SimPowerSystem/Simulink toolbox in the MATLAB software environment. During the simulation time, it is assumed that the ambient temperature is constant at 25°c and the irradiance changes, as depicted in Fig. 8a. At the startup of the system under study, the Y-connection load is not connected, and later at t=2.25 s, this load is connected to the PCC. Furthermore, to apply an unbalanced load to the system, phase C of Y-connection load is open circuited at t=2.75 s, which leads an unbalanced PCC voltage.

Table 3. Control system parameters

Parameter	value
k_{pd}^{+}, k_{pq}^{+}, k_{pd}^{-}, k_{pq}^{-}	0.39
k_{id}^{+}, k_{iq}^{+}, k_{id}^{-}, k_{iq}^{-}	3.63
G_{ff} (s)	$\frac{1}{0.002s+1}$
$k_{pv\text{-}d}^{-}$, $k_{pv\text{-}q}^{-}$	1.5
k_{p_vac}	1
k_{i_vac}	2e6
G_v (s)	$\frac{1868(s+19)}{s(s+2077)}$

Figures 8 to 14 illustrate the obtained results. Fig. 8 shows the obtained results for the DC part of the studied system. The output power of PV and DC link voltage are shown in Fig. 8b and 8c, respectively. It can be seen that the changes in irradiance have a direct effect on the PV output power. The power value of 2.86 MW at the time of maximum irradiance reaches 1.41 MW for irradiance 524 W/m^2. Additionally, Fig. 8c shows that DC link voltage is well regulated despite irradiance changes. In addition, Fig. 8b illustrates that the proposed strategy for unbalanced voltage compensation does not affect the PV system performance. However, after unbalanced load connection is fluctuated at =2.75 s, the DC link voltage components by the inverter due to the production and injection of negative sequence.

The positive and negative sequence components of the inverter output voltage and current at d and q axis are presented in Fig. 9. As can be seen, the positive sequence component of PCC voltage in d-axis is well controlled and follows its reference (391 V). In addition, the positive sequence component of PCC voltage in q-axis is zero due to the PLL function. As a result, the changes in irradiance do not affect the performance of AC voltage control system. Furthermore, as can be seen in Fig. 9, the waveform of positive sequence component of inverter current in d-axis is similar to PV power because with the constant V_d^+ and $V_q^+ = 0$, the output power is directly controlled by I_d^+. The negative sequence components of the inverter current are negligible before unbalanced load connection. However, after t = 2.75 s, the negative sequence currents are injected to compensate for the unbalanced voltage.

The inverter output currents and three-phase voltages at PCC are shown in Fig. 10 and Fig. 11, respectively. Fig. 11 depicts that the unbalanced PCC voltage is appropriately compensated and regulated.

According to the IEC standard, VUF should be less than 2% [30]. This factor is actually obtained by dividing the negative sequence voltage by the positive sequence voltage. Fig. 12 shows the VUF of PCC voltage. As can be seen, the VUF is about 6.1% at t = 2.78s, and its value falls within permissible limit (2%) after about 0.4s. In addition, the VUF reaches a value of 0.18% at t = 4s. Fig 13 presents the FFT analysis results. As shown in Fig. 13a, after balanced load connection, the Total Harmonic Distortion (THD) of PCC voltage is 0.29%. According to Fig. 13b, after unbalanced voltage compensation the value of THD is 0.77%. The amount of THD and VUF are summarized in Table 4. As one can see, the simulation results confirm the effectiveness of the proposed control strategy for unbalanced voltage compensation.

Fig. 14 illustrates the active power flow in the AC side. As can be seen, before load connection, the PV power is injected into the grid. The three-phase load is connected to the PCC at t = 2.25s and imposes 2.16 MW. Due to the downward trend of the output power of the inverter, the rest of the load power is supplied by the grid. As the PV power increases, the grid power decreases consequently. By unbalanced load connection at t = 2.75s, due to disconnection of phase C of Y-connection load, the amount of load active power decreases to approximately 1 MW. As the PV power is increased, the load is supplied and the rest of the active power is injected into the grid.

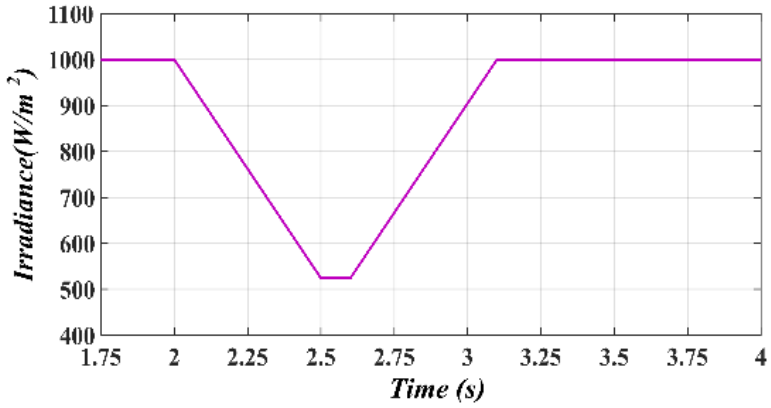

a)

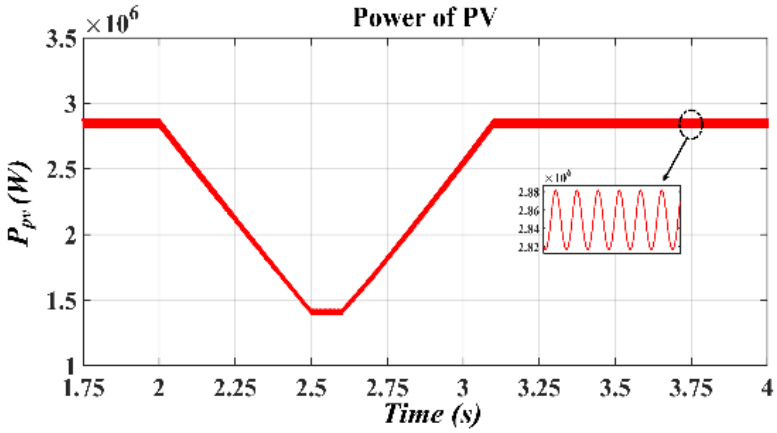

b)

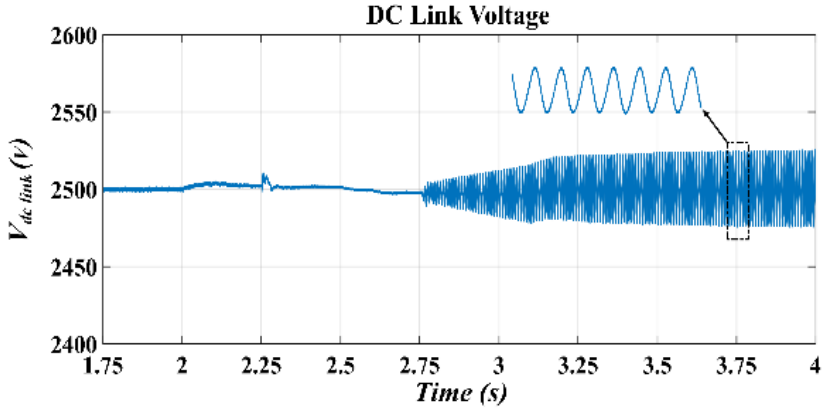

c)

Fig. 8. a) Irradiance b) PV power c) DC link voltage

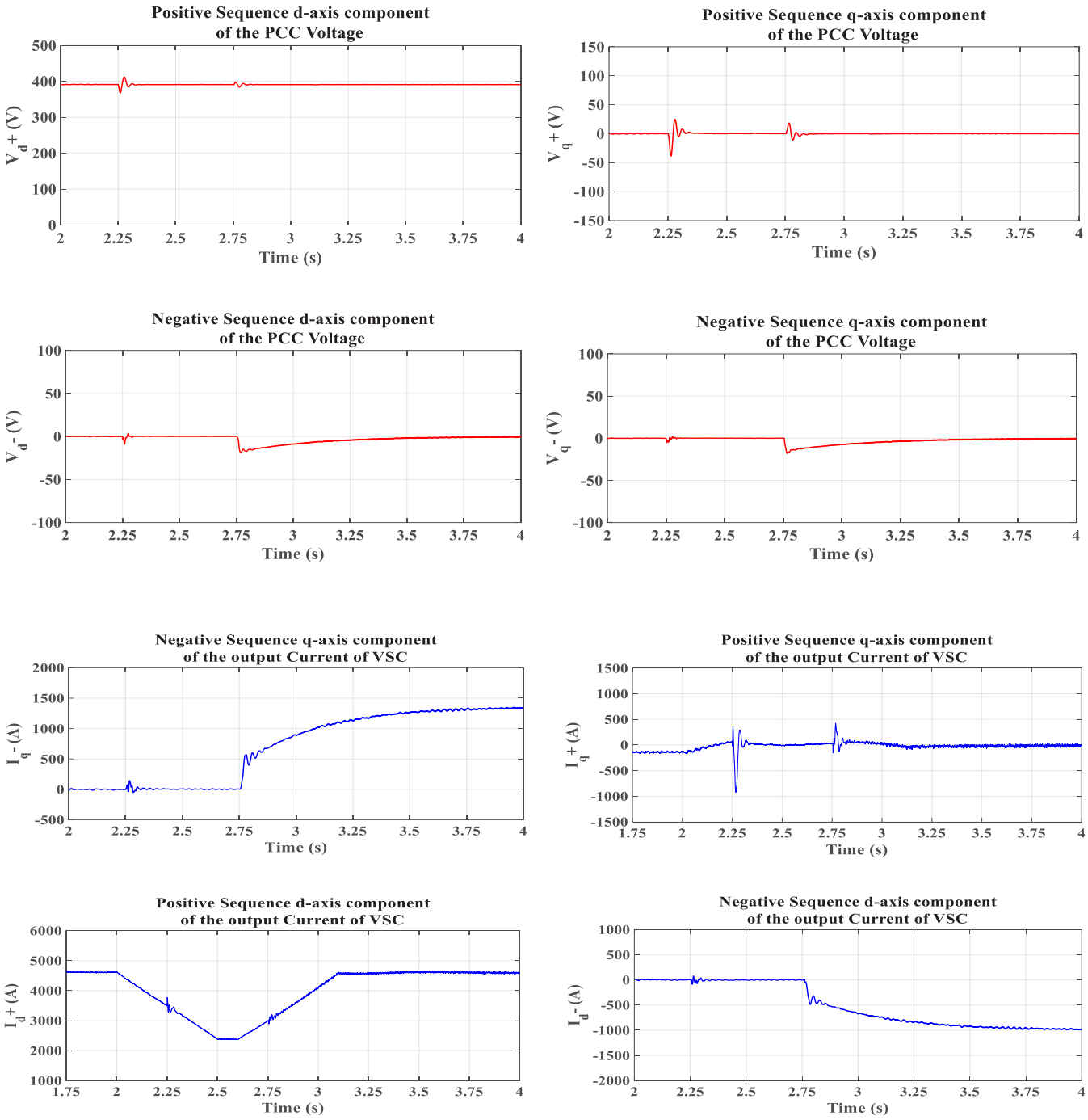

Fig. 9. Positive and negative sequence components of inverter output voltage and current at d and q axis

Table 4. THD and VUF of PCC voltage

Parameter	After applying a balanced load	After applying an unbalanced load
THD (%)	0.29	0.77
VUF (%)	< 0.1	0.18

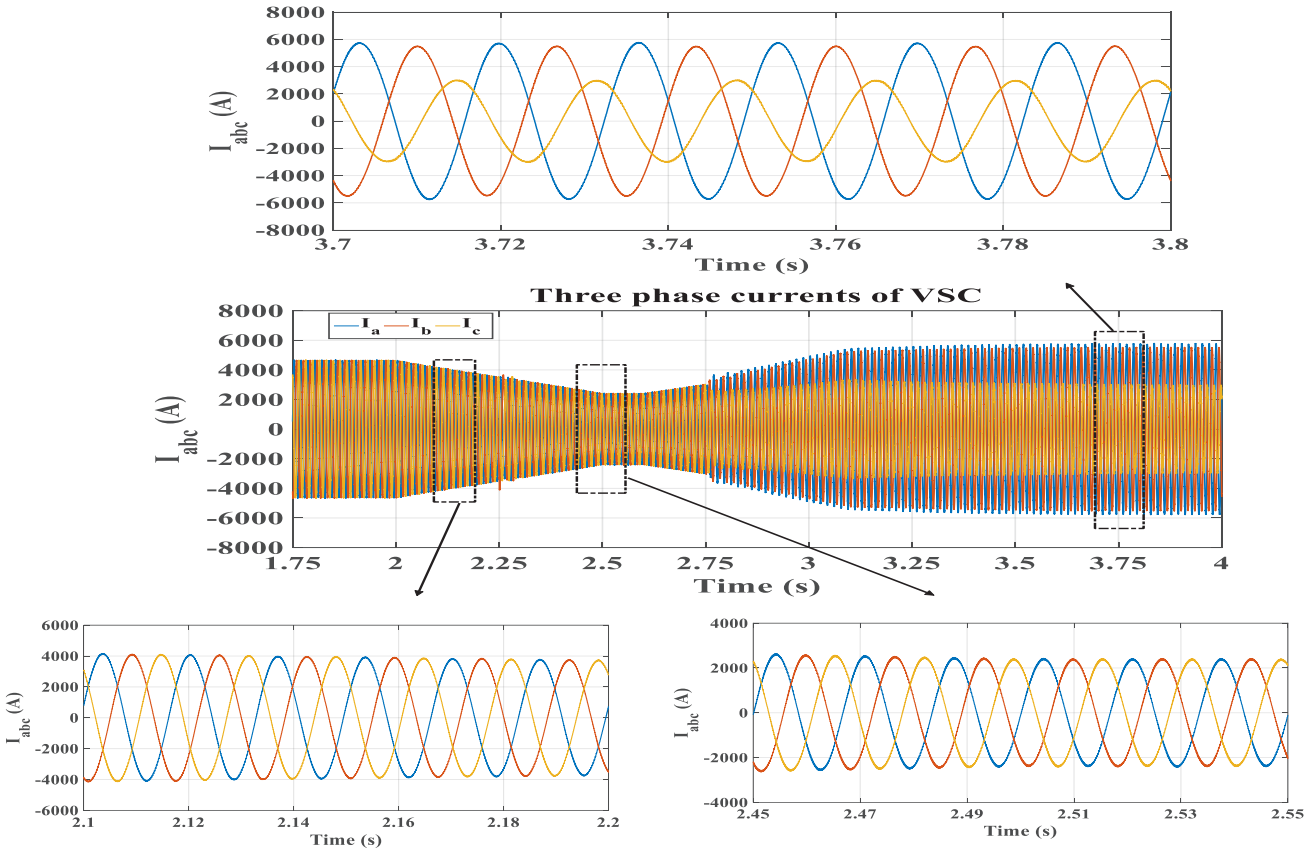

Fig. 10. the inverter output currents

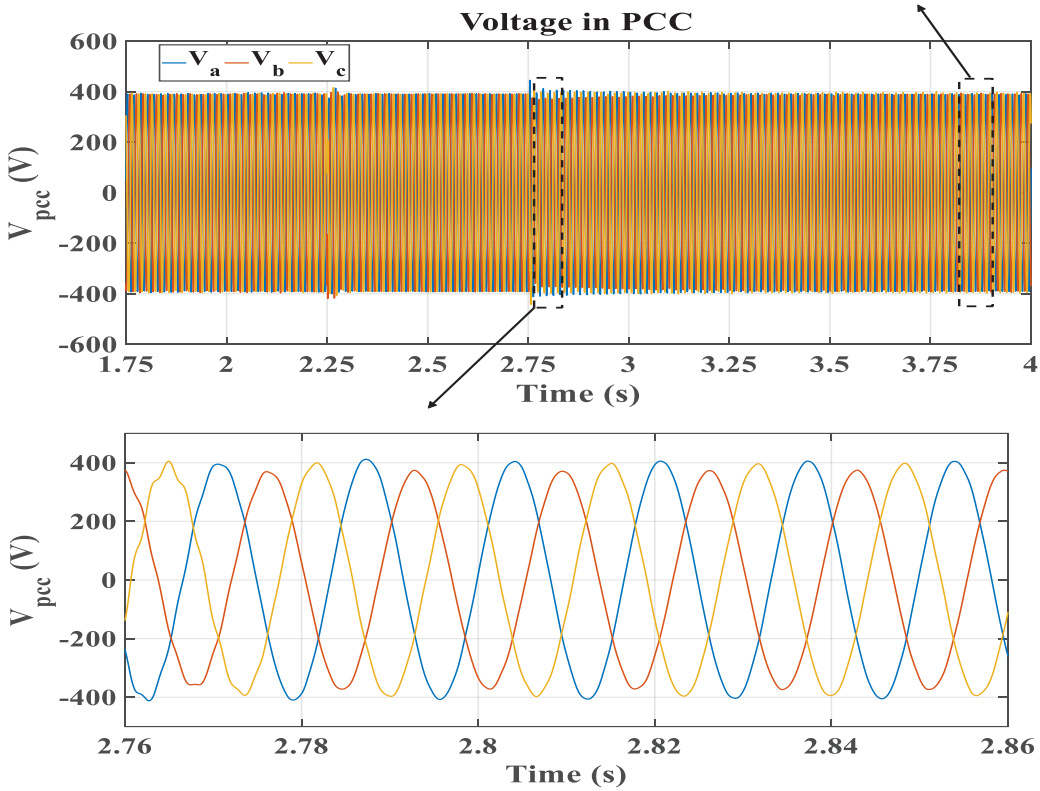

Fig. 11. PCC voltage

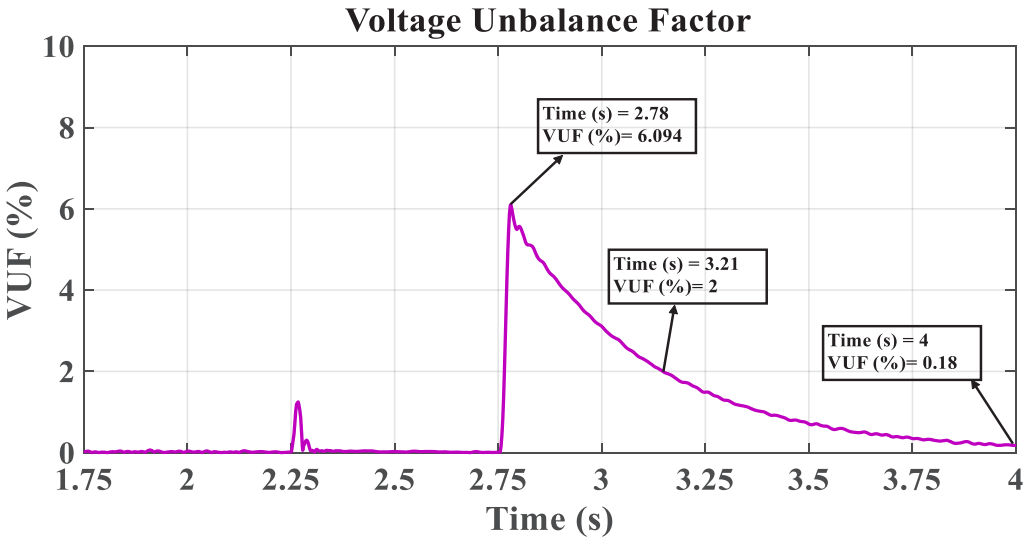

Fig. 12. the Voltage Unbalance Factor (VUF) of PCC voltage

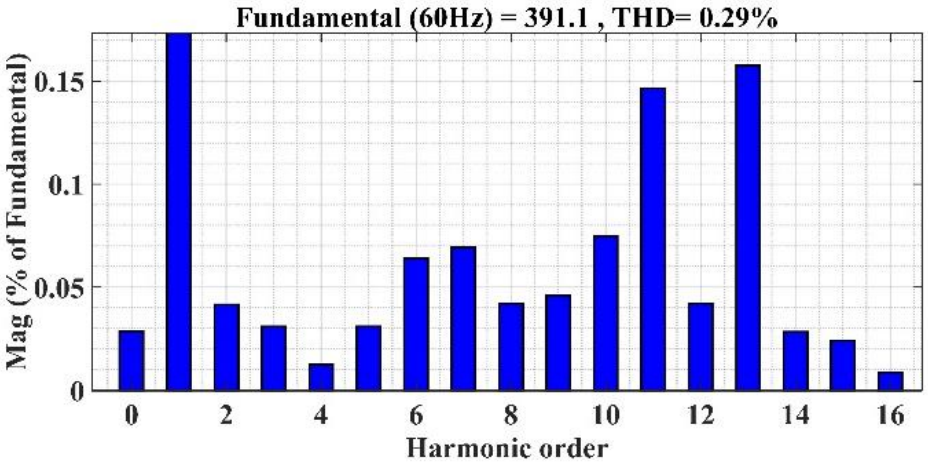

a)

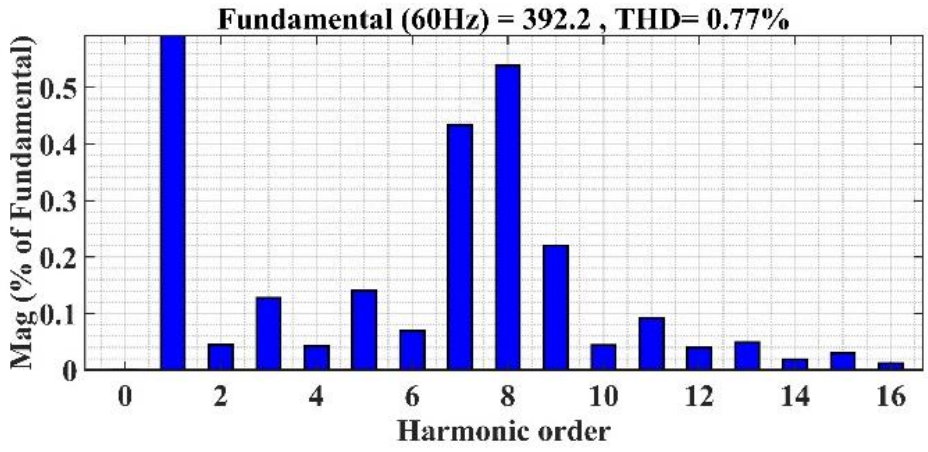

b)

Fig. 13. THD of PCC voltage a) under balanced load b) under unbalanced load

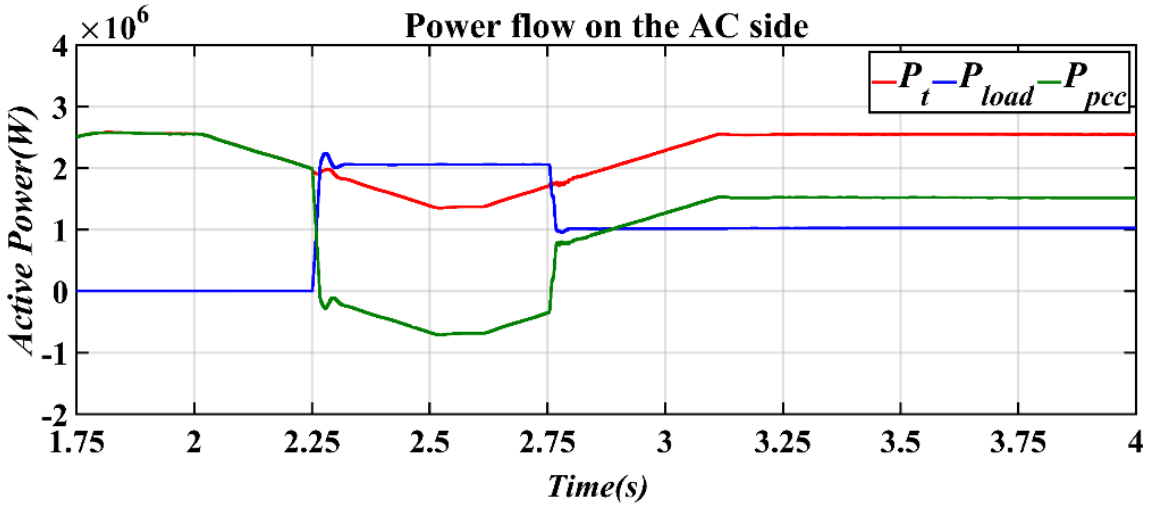

Fig. 14. Active power flow in the AC side

5- Conclusion

This paper presents an effective control method for two-stage grid-connected Photovoltaic system to compensate for unbalanced voltage at PCC caused by unbalanced loads. To appropriately separate the sequence components of voltage and current signals, DDSRF has been proposed. Despite the dynamic and intermittent nature of the PV system, the proposed control system properly controls DC link voltage and PV output power. Using the proposed control strategy, VUF at the PCC falls within its permissible range (2%), and THD of PCC voltage remains less than 1%. As a result, this paper shows that the grid-connected Photovoltaic system can be used as a grid-support for PCC voltage regulation and unbalanced voltage compensation.

6- Nomenclature

$G_{ff}(s)$ Feed forward filter in the current control loop

$i_{\alpha\beta}^{+}$ positive sequence $\alpha\beta$ components of the inverter current

$i_{\alpha\beta}^{-}$ negative sequence $\alpha\beta$ components of the inverter current

i_{dq}^{+} positive sequence dq components of the inverter current

i_{dq}^{-} negative sequence dq components of the inverter current

$\bar{i}_{dq}^{+}$ DC term of positive sequence dq components of the current

$\bar{i}_{dq}^{-}$ DC term of negative sequence dq components of the current

$\tilde{i}_{dq}^{+}$ AC term of positive sequence dq components of the current

$\tilde{i}_{dq}^{-}$ AC term of negative sequence dq components of the current

k_{pdq}^{+} Proportional controller coefficient of the positive current control loop

k_{pdq}^{-} Proportional controller coefficient of the negative current control loop

k_{idq}^{+} Integral controller coefficient of the positive current control loop

k_{idq}^{-} Integral controller coefficient of the negative current control loop

k_{p-vac} Proportional controller coefficient of the PCC voltage control loop

k_{i-vac} Integral controller coefficient of the PCC voltage control loop

k_{pv-dq}^{-} Proportional controller coefficient of the negative control loop for unbalanced voltage compensation

$v_{\alpha\beta}^{+}$ positive sequence $\alpha\beta$ components of the voltage

$v_{\alpha\beta}^{-}$ negative sequence $\alpha\beta$ components of the voltage

v_{dq}^{+} positive sequence dq components of the voltage

v_{dq}^{-} negative sequence dq components of the voltage

$\bar{v}_{dq}^{+}$ DC term of positive sequence dq components of the voltage

$\bar{v}_{dq}^{-}$ DC term of negative sequence dq components of the voltage

$\tilde{v}_{dq}^{+}$ AC term of positive sequence dq components of the voltage

$\tilde{v}_{dq}^{-}$ AC term of negative sequence dq components of the voltage

Greek symbols

θ angular displacement

τ_i time constant of the current controller

ω angular frequency

References

[1] A. Datta, R. Sarker, I. Hazarika, An efficient technique using modified p–q theory for controlling power flow in a single-stage single-phase grid-connected PV system, IEEE Transactions on Industrial Informatics, 15(8) (2018) 4635-4645.

[2] Pirzadi, M. and A.A. Ghadimi, Performance evaluation of first Iranian large scale Photovoltaic power plant. AUT Journal of Electrical Engineering, 2020. 52(1): p. 19-30.

[3] M.H. de Freitas Takami, S.A. Oliveira da Silva, L.P. Sampaio, Dynamic performance comparison involving grid-connected PV systems operating with active power-line conditioning and subjected to sudden solar irradiation changes, IET Renewable Power Generation, 13(4) (2019) 587-597.

[4] You, R. and X. Lu, Voltage unbalance compensation in distribution feeders using Soft Open Points. Journal of Modern Power Systems and Clean Energy, 2022

[5] V.L. Srinivas, B. Singh, S. Mishra, Fault ride-through strategy for two-stage grid-connected Photovoltaic system enabling load compensation capabilities, IEEE Transactions on Industrial Electronics, 66(11) (2019) 8913-8924.

[6] Y. Lu, K. Sun, H. Wu, X. Dong, Y. Xing, A three-port converter based distributed DC grid connected PV system with autonomous output voltage sharing control, IEEE Transactions on Power Electronics, 34(1) (2018) 325-339.

[7] Wu, F., et al., Inertia and damping analysis of grid-tied Photovoltaic power generation system with DC voltage droop control. IEEE Access, 2021. 9: p. 38411-38418.

[8] T.A. Naidu, S.R. Arya, R. Maurya, Multiobjective dynamic voltage restorer with modified EPLL control and optimized PI-controller gains, IEEE Transactions on Power Electronics, 34(3) (2018) 2181-2192.

[9] M. Pradhan, M.K. Mishra, Dual $ P $-$ Q $ theory based energy-optimized dynamic voltage restorer for power quality improvement in a distribution system, IEEE Transactions on Industrial Electronics, 66(4) (2018) 2946-2955.

[10] A.P. Torres, P. Roncero-Sanchez, V.F. Batlle, A two degrees of freedom resonant control scheme for voltage-sag compensation in dynamic voltage restorers, IEEE Transactions on Power Electronics, 33(6) (2017) 4852-4867.

[11] S. Devassy, B. Singh, Control of a solar Photovoltaic integrated universal active power filter based on a discrete adaptive filter, IEEE Transactions on Industrial Informatics, 14(7) (2017) 3003-3012.

[12] F. Wang, J.L. Duarte, M.A. Hendrix, Grid-interfacing converter systems with enhanced voltage quality for microgrid application—Concept and implementation, IEEE Transactions on power electronics, 26(12) (2011) 3501-3513.

[13] S.K. Dash, P.K. Ray, Power quality improvement utilizing PV fed unified power quality conditioner based on UV-PI and PR-R controller, CPSS Transactions on Power Electronics and Applications, 3(3) (2018) 243-253.

[14] M. Castilla, J. Miret, A. Camacho, J. Matas, L.G. de Vicuña, Voltage support control strategies for static synchronous compensators under unbalanced voltage sags, IEEE transactions on industrial electronics, 61(2) (2013) 808-820.

[15] T.-L. Lee, S.-H. Hu, Y.-H. Chan, D-STATCOM with positive-sequence admittance and negative-sequence conductance to mitigate voltage fluctuations in high-level penetration of distributed-generation systems, IEEE Transactions on Industrial Electronics, 60(4) (2011) 1417-1428.

[16] M. Yao, I.A. Hiskens, J.L. Mathieu, Mitigating voltage unbalance using distributed solar Photovoltaic inverters, IEEE Transactions on Power Systems, 36(3) (2020) 2642-2651.

[17] M. Savaghebi, A. Jalilian, J.C. Vasquez, J.M. Guerrero, Secondary control scheme for voltage unbalance compensation in an islanded droop-controlled microgrid, IEEE Transactions on Smart Grid, 3(2) (2012) 797-807.

[18] F. Nejabatkhah, Y.W. Li, B. Wu, Control strategies of three-phase Distributed Generation inverters for grid unbalanced voltage compensation, IEEE Transactions on Power Electronics, 31(7) (2015) 5228-5241.

[19] M. Hamzeh, H. Karimi, H. Mokhtari, A new control strategy for a multi-bus MV microgrid under unbalanced conditions, IEEE Transactions on Power Systems, 27(4) (2012) 2225-2232.

[20] L. Meng, F. Tang, M. Savaghebi, J.C. Vasquez, J.M. Guerrero, Tertiary control of voltage unbalance compensation for optimal power quality in islanded microgrids, IEEE Transactions on Energy Conversion, 29(4) (2014) 802-815.

[21] C. Lascu, L. Asiminoaei, I. Boldea, F. Blaabjerg, High performance current controller for selective harmonic compensation in active power filters, IEEE Transactions on Power electronics, 22(5) (2007) 1826-1835.

[22] H.-S. Song, K. Nam, Dual current control scheme for PWM converter under unbalanced input voltage conditions, IEEE transactions on industrial electronics, 46(5) (1999) 953-959.

[23] N.R. Merritt, C. Chakraborty, P. Bajpai, New voltage control strategies for VSC-based DG units in an unbalanced microgrid, IEEE Transactions on Sustainable Energy, 8(3) (2017) 1127-1139.

[24] P. Mishra, A.K. Pradhan, P. Bajpai, Voltage control of PV inverter connected to unbalanced distribution system, IET Renewable Power Generation, 13(9) (2019) 1587-1594.

[25] M. Reyes, P. Rodriguez, S. Vazquez, A. Luna, R. Teodorescu, J.M. Carrasco, Enhanced Decoupled Double Synchronous Reference Frame current controller for unbalanced grid-voltage conditions, IEEE Transactions on power electronics, 27(9) (2012) 3934-3943.

[26] M. Ahmadi, S. Karimi, Voltage unbalance compensation using new structure of decouple double synchronous reference frame in stand-alone microgrids, IET Generation, Transmission & Distribution, 14(22) (2020) 5093-5103.

[27] P. Rodríguez, J. Pou, J. Bergas, J.I. Candela, R.P. Burgos, D. Boroyevich, Decoupled Double Synchronous Reference Frame PLL for power converters control, IEEE Transactions on Power Electronics, 22(2) (2007) 584-592.

[28] A. Yazdani, R. Iravani, Voltage-sourced converters in power systems: modeling, control, and applications, John Wiley & Sons, 2010.

[29] 305 Solar panel exceptional efficiency and performance, SPR-305-WHT, in, sunpowercorp.com, 2007.

[30] J.M. Guerrero, P.C. Loh, T.-L. Lee, M. Chandorkar, Advanced control architectures for intelligent microgrids—Part II: Power quality, energy storage, and AC/DC microgrids, IEEE Transactions on industrial electronics, 60(4) (2012) 1263-1270.

HOW TO CITE THIS ARTICLE

A. Mohammadi, Sh. Karimi, H. Moradi Cheshmehbeigi, Unbalanced Voltage Compensation Using Grid-Connected Photovoltaic System , AUT J. Elec. Eng., 54(2) (2022) 295-312.

DOI: 10.22060/eej.2022.21387.5472